Effect of Shot Peening Parameters on the Properties of Surface Layers in AISI 4140 in Different Heat Treatment Conditions

by H. Hozapfel, A. Wick, and O. Vöhringer

Abstract

The effects of the technical important shot peening parameters peening pressure, mass flow, hardness and size of the shot particles on the surface layer properties were systematically studied. Samples of the differently heat treated steel AISI 4140 (German Grade 42CrMo4) with a hardness between HV 230 and HV 660 were shot peened. The surface layers were characterized by measuring the residual stresses and the half width values of interference lines using X-ray diffraction and by determining the surface roughness. With increasing workpiece hardness characteristic maxima of the compressive residual stresses beneath the surface are observed. An increasing peening intensity causes a deeper penetration of the compressive residual stresses. During shot peening the half values near the surface increase for softer material conditions, whereas these values decrease for harder material conditions. This is caused by a multiplication of dislocations in the softer material and by a rearrangement of dislocations of high density to energetically more favorable positions in the harder material.

1. Introduction

Shot peening is an often used industrial process to improve the component properties, especially fatigue life and fatigue strength. This is caused in soft material conditions by work hardening of the near surface layers, which prevents or reduces the probability of crack formation in this area. With increasing hardness of the material the amounts and the penetration depth of the compressive residual stresses become more substantial, thus preventing or reducing crack formation [1, 2].

For an optimization of the shot peening process it is necessary to know the effects of the shot peening parameters. The result of the shot peening treatment is influenced by the machining parameters, the shots used and the workpiece that is shot peened. The technically most important parameters are the shot velocity [3-8], the mass flow or exposure time [3, 4, 9, 14], the hardness and size of the shots [3, 4, 6, 9, 15-22] and the workpiece hardness [23-25].

Although, there are already some papers about the effects of these parameters, there does not exist any systematical study on the separated influence of these properties, especially on the induced residual stresses and the surface work hardening.

This paper reports on the influence of the parameters peening pressure, mass flow, hardness and size of the shots and workpiece hardness on the properties of the surface layers of AISI 4140 (German Grade 42CrMo4) steel samples in different heat treatment conditions. The surface layers are characterized by the distribution of residual stress and half width values of the interference lines determined by X-ray measurement. In this context, the half width value is a measure of the microstructural work hardening or work softening of the material. Another property to characterize the surface is the surface roughness R_t.

2. Material and Heat Treatment

The investigations were carried out on the heat treatable AISI 4140 (German Grade 42CrMo4) with the chemical composition 0.44 C, 1.05 Cr, 0.21 Mo, 0.22 Si, 0.59 Mn, 0.06 Ni, 0.02 P, 0.01 S, bal Fe (in wt.-%). Flat samples with the dimensions 110 x 24 x 2 mm^3 were machined. The parameters of the heat treatments which were carried out in a vacuum furnace (Fa. Degussa) are summarized in Tab. 1.

3. Experimental Details

All shot peening treatments were carried out simultaneously from both sides using an air blast machine (Fa. Baiker). The nozzles had a diameter of 8 mm. The distance z between nozzle and sample was always z = 80 mm and the peening angle was 90°. For the parameter variation, the peening pressure laid between 1.6 and 8 bar and the mass flow between 1.5 and 10 kg/min. For the variation of the shot type, S110 46HRC, S170 46HRC, S170 56HRC and S330 56HRC were used. The average diameter of the shots is 0.28 mm for S110, 0.43 mm for S170 and 0.84 mm for S330. To reduce the shot deformation and wear, S17 56HRC was used for the peening pressure and mass flow variation for the hardened, the hardened and at 180°C tempered (T180) and the hardened and at 300°C tempered (T300) conditions. For the larger mass flows, a peening pressure of 3 bar was chosen to prevent the hoses from plugging.

The residual stresses were determined using the $\sin^2\psi$-method [26] with a CrKα-radiation on the {211}-interference plane. The residual stress and half width value measurements at the subsurface layers were carried out after removing thin layers with an electrolytical polishing technique, in steps of 0.025 mm to a depth of 0.4 mm. The measured residual stress distributions were corrected for the surface removement applying the method according to [11].

4. Results

4.1 Influence of workpiece hardness

The influence of the workpiece hardness on the surface properties after shot peening at constant peening parameters was studied at six different heat treatment conditions which are shown in Tab. 2.

Fig. 1 presents the surface roughness R_t after shot peening as a function of workpiece hardness. For the normalized condition R_t increases by a factor of 10. For the hardened condition the surface roughness is almost the same for both the peened and the unpeened samples.

The residual stress distribution of the shot peened samples can be seen from Fig. 2, showing an increasing amount of residual stresses at the direct surface layer for the normalized condition up to the tempered condition T450. With increasing sample hardness the residual stresses at the surface decrease. The penetration depth of the compressive residual stresses decreases with increasing workpiece hardness. Only the T180 condition (600 HV) shows a smaller penetration depth than the hardened condition (660 HV). For increasing sample hardness a characteristic maximum of compressive residual stresses can be found below the surface, in a depth of 0.05 mm and a relative maximum at the surface. Its value amounts to $\sigma^{rs} = -800$ N/mm^2.

In Fig. 3 the half width distributions as a function of the distance from surface for the different heat treated samples after shot peening can be seen. The curves for the normalized and the hardened and at 650°C tempered samples (T650) are similar. However, the half width values for the normalized condition are somewhat smaller than those for the T650. Both curves show increasing values at the surface. The half width values for T450 are constant. After shot peening, in the case of T180, T300 and the hardened conditions half width values in the area close to the surface are smaller than those measured in deeper regions of the sample. There is a minimum beneath the surface nearby 0.05 mm and a relative maximum at the surface, respectively.

4.2 Influence of shot type

The influence of the shot type was studied at six different heat treatment conditions. Four different shots were used. The other peening parameters, that can be seen in Tab. 3, were held constant.

Fig. 4 presents the surface roughness R_t of the samples after shot peening, which increases with decreasing sample hardness for all shot types. If shot size and hardness increase, the surface roughness rises for all heat treatment conditions. The softer the conditions, the more obvious the differences are.

The influence of the shot type on the residual stress distribution can be seen for the hardened and tempered condition T450 in Fig. 5 and for the hardened condition in Fig. 6. For the condition T450 the penetration depth of the compressive residual stresses increases with the shot diameter, whereas the residual stresses up to a depth of 0.1 mm beneath the surface are not effected. For a constant shot size, the hardness of the shots has no influence on the residual stress distribution.

For the hardened condition the penetration depth of the residual stresses also increases with the shot diameter. Besides this, the distance from the surface of the maximum value of compressive residual stresses increases. Contrary to the T450 condition, the maximum of the compressive residual stresses increases with the shot hardness for the hardened workpiece condition. However, the distance from surface of this the maximum is not effected. Shot diameter and hardness have no significant influence on the half width values for all heat treatment conditions.

4.3 Influence of the peening pressure

Tab. 4 represents the peening parameters for the peening pressure variation. The shot S170 46HRC was used for the normalized as well as for the T650 and T450 condition. The harder workpiece conditions were peened with the shot S170 56HRC to avoid shot deformation and wear.

The influence of the peening pressure on the surface roughness R_t is described in Fig. 7 for the different heat treatment conditions. For the normalized and the T650 conditions the surface roughness increases up to the maximum peening pressure p = 8 bar. The surface roughness of r the T450 and T300 conditions first of all increases with p and R_t and is constant for peening pressures above p = 5 bar. The surface roughness of the T180 and the hardened conditions is not significantly affected by the peening pressure.

The residual stress distributions for different peening pressures were measured for the normalized and the hardened conditions. For the normalized condition the values of the compressive residual stresses and the penetration depth shown in Fig. 8 are higher for the peening pressure p = 5 bar in comparison to p = 1.6 bar. The surface values of the residual stresses, however, are almost identical. No substantial changes in the residual stress distributions are recognized for the peening pressures 5 bar and 8 bar.

As for the other conditions, the surface values of the residual stresses for the hardened condition are independent of the peening pressure (Fig. 9). The distance from the surface of the penetration depth and the maximum compressive residual stress increase with increasing peening pressure, however, the value of the maximum is almost constant.

The half width values for this workpiece condition is shown in Fig. 10 together with the findings of the normalized and the T450 conditions. For the normalized condition, an increase of the peening pressure to 5 bar results in an increase of the half width value of 0.4 °2θ. The curves for 5 bar and 8 bar do not show any marked differences. There is no influence of the peening pressure on the half width values for the T450 condition. An increase of the peening pressure leads to a decrease of the half width values for the hardened condition up to a surface distance of 0.275 mm. A peening pressure of 8 bar affects a further decrease of the half width values compared to the curve for p = 5 bar.

4.4 Influence of the mass flow

The mass flow variation was carried out for the investigations using the peening parameters shown in Tab. 5. As before, the harder material conditions (T300, T180, hardened) were peened with the shot S170 56HRC.

In Fig. 11 the surface roughness values for the different material conditions are shown as a function of the mass flow m. For the normalized and the V650 conditions the surface roughness is decreasing with increasing mass flow. For harder workpiece conditions the decrease of the surface roughness diminishes. For all conditions, however, the surface roughness for m = 10 kg/min is smaller than the one for m = 1.5 kg/min.

The effect of the mass flow variation on the residual stress distribution is shown for the T450 (Fig. 12) and the hardened (Fig. 13) conditions. For the T450 condition the mass flow has no significant influence on the compressive residual stresses

up to a surface distance of 0.1 mm. At large distances from the surface the compressive residual stresses decrease with increasing mass flow, connected with a reduction of the penetration depth of the compressive residual stresses.

The curves for the hardened condition (Fig. 13) show a constant surface value of the residual stresses. With an increase of the mass flow from 1.5 kg/min to 6 kg/min the maximum value of the compressive residual stress is increasing. The maximum value for a mass flow of 10 kg/min lies between those for 1.5 kg/min and 6 kg/min. The distance from surface, where the maximum is found is constant for all mass flows. For surface distances larger than 0.125 mm the compressive residual stresses for higher m-values are always smaller than for a mass flow of m = 1.5 kg/min. Therefore, the penetration depth of the compressive residual stresses decrease slightly with increasing mass flow.

5. Discussion

The results which are presented in chapter 4.1 for different heat treatment conditions at constant peening parameters confirm the model [23] that describes the residual stress formation during shot peening. The maximum value of the compressive residual stresses of the normalized condition, which shows the smallest hardness (230 HV) of the materials investigated, can be found directly on the surface. This finding is explained in [23] by the dominating hammering effect of the shots, which causes the highest amount of plastic deformation on the surface. The location of the maximum compressive residual stress, however, is beneath the surface for the T300, T180 and the hardened conditions, which can be explained by the dominating effect of the Hertzian stress. The Hertzian stress causes a maximum shear stress below the surface. If this stress is greater than the local materials resistance for the onset of plasticity, inhomogeneous plastic deformation and the formation of compressive residual stresses develop. For the T450 and T300 conditions (Fig.2), which have a hardness of 430 HV and 525 HV, the values of the compressive residual stresses have their highest amount directly at the surface. For the harder workpiece conditions, the residual stresses are reduced starting from the maximum value with decreasing distance from surface. The maximum value of the compressive residual stresses increases with increasing workpiece hardness up to the T180 condition (600 HV), however, slightly decreases for the hardened condition (660 HV). This behaviour can be explained in this connection with the course of the penetration depth, which, as demanded in the model [23], decreases with increasing workpiece hardness or, more exactly, with increasing material resistance against the onset of plasticity. An exception in this case is the T180 condition, however, where the minimum value of the penetration depth is reached at a hardness which is smaller than for the hardened condition. However, in this case the 0.01-proof stress is larger in the T180 condition than in the hardened condition due to the pinning of dislocations by the solute carbon atoms and by fine carbide precipitations [28]. This work hardening effect can not be detected in hardness measurements, because the plastic deformation caused by the hardness pyramid is so large that all moveable dislocations are broken away from their pinning points.

The half width values are a measure of the microstructural work hardening changes in the surface layers. In Fig. 3 it can be recognized, that the half width values increases in the surface layers compared to the values in deeper regions of the sample. This indicates microstructural work hardening effects due to the peening induced multiplication of dislocations [24]. In contrast to this behaviour, the half width values decreases in the surface layers in the case of harder workpiece conditions (HV > 500). This indicates in conditions with very high dislocation densities before peening that a microstructural softening process occurs, caused by a rearrangement of dislocations in energetical more favorable positions combined with reduced mean microstrains as well as by annihilation of dislocations. Furthermore, in hardened conditions stress induced rearrangement of soluted carbon atoms can rearrange during peening into octahedral sites of less lattice deformation due to the Snoek-effect can contribute also to the decrease of the half width values [24]. In case of the T450 condition the half width values do not change by shot peening. This indicates that the work hardening effect due to dislocation generation and the work softening effect due to dislocation annihilation and rearrangement balance each other.

For soft and medium hard workpiece conditions (HV<300 and 300<HV<600, resp.) the variation of the shot hardness from 46HRC (460HV) to 56HRC (620HV) has no influence on the distribution of the residual stresses. This finding is in contrast to the results of [22], where for a 1%-chromium spring steel (German Grade 50Cr4) with a hardness of 420HV for an increase of the shot hardness from 450HV to 600HV, increasing residual stresses and an increasing distance from the surface of the maximum value of the compressive residual stress were measured. This finding can be explained using the results of [29], where the influence of the shot hardness on the deformation depth was studied and a direct proportionality of the deformation depth and the shot hardness was found. If the shot is much harder than the workpiece, it is called rigid. An even harder shot does not increase the deformation depth any further. However, in this context, the shot velocity is important, because it has strong influence on the deformation depth. The higher the shot velocity is, the more the deformation depth increases with increasing shot hardness. Therefore a comparison between the presented results and the findings of [22] is not possible, especially since the studies in [22] were carried out with a centrifugal type machine with other shot velocities than an air blast machine. For the harder workpiece conditions (HV>600) the increase of the shot hardness results in an increase of surface residual stresses and the maximum value of the compressive residual stresses. The distance from surface of the maximum, however, is not affected. This behaviour is in agreement with [2] and the studies of [9, 15].

With increasing shot size the penetration depth of the residual stresses is increasing for all heat treatment conditions at constant shot hardness. For the hard conditions in addition to this finding, the maximum of the compressive residual stresses, which is constant, is moving further away from the surface. The increase of the penetration depth and of the distance from surface of the maximum value can be explained by the larger mass of the single balls, which increases the impulse of the shots. This enlargement of the shot impulse also causes a larger plastification of the direct surface layer. Larger plastification are also increasing the thickness of the penetrated layers. This effect can shift the residual stress distribution over the cross section in such a

manner that the surface residual stresses are not significantly changed.

In all the material conditions an increasing peening pressure causes a larger penetration depth of the compressive residual stresses which is in agreement with the results in [3-8]. Thereby the surface residual stresses are constant, where other investigations report as well of an increase [6] as of a decrease due to overpeening by multiple coverage. The constant residual stresses at the surface can be explained by the same effect mentioned for the variation of the shot size. At the harder workpiece conditions the shifting of the maximum value of the compressive residual stresses is caused by the location of the maximum shear stress which can be found at $z = 0.47a$ (a = half the width of the shot impact). When the peening pressure is increased, the surface roughness increases as a sign of larger shot impacts which is connected with an increase of z.

An enlargement of the peening pressure effects an increase of the half width values in the surface layers due to a larger plastification in the surface layers and an enlargement of the dislocation density in this region. However, for the harder workpiece conditions the half width values in the near surface layers are decreasing with increasing peening pressure. In this case the dislocations with high density which were generated in the material by hardening and reduced only moderately at tempering at lower temperatures by recovery processes can rearrange during peening into energetic more stable configurations with reduced mean microstrains.

An enlargement of the mass flow yields for all material conditions a decrease of the penetration depth of the compressive residual stresses. Due to the fact that the probability of mutual pushes of the shots in the nozzles and the hoses increases with the mass flow. Thereby a decrease of the kinetic energy stored in the shots occurs which causes a smaller penetration depth of the compressive residual stresses. For the softer material conditions the mass flow has no influence on the surface residual stresses. For the harder conditions, however, the maximum value of the residual stresses is first increasing for mass flows between 1.5 kg/min and 6 kg/min and then decreasing for mass flows between 6 kg/min and 10 kg/min. The reason for this phenomena is the coverage which is below 100% for small mass flows. An increase of the mass flow causes an increasing maximum residual stress value, as long as a 100% coverage is reached. A further increase of the mass flow effects a decrease of the residual stress as described above. At first sight, these results are contradictory to other investigations [4, 9, 16], where an increase of the mass flow is considered to be equivalent to an increasing coverage. An increase of the coverage, however, can be reached not only with an increasing mass flow but also with prolongation of the exposure time which can be realized for an air blast system with a decreasing nozzle velocity. In Fig. 14 a comparison of the residual stress distribution after shot peening with the same coverage for normalized samples can be seen. One sample was shot peened with a mass flow of 10 kg/min and an exposure time of $t = 16$ s. The other was peened with a mass flow of 1.5 kg/min and theoretical exposure time of $t = 106$ s. Under the latter conditions the penetration depth becomes larger. Therefore, an increase of the coverage via the mass flow can cause other residual stress distributions than an increase via the exposure time. A comparison of these findings and the results of other investigations is problematic because there the coverage was determined by the exposure time.

The penetration depth of the residual stresses and the depth where the half width values reach the values of an unpeened sample do not always correspond with each other. Obviously, different processes are responsible for the change of the residual stresses and the half width values. The compressive residual stresses result from a plastification of the surface layers balancing the residual stresses over the entire cross section of a sample. Therefore, the penetration depth of the compressive residual stresses does not necessarily correspond to the depth of the plastification. The half width value on the other hand is effected by microstructural processes (dislocation multiplication or dislocation rearrangement in energetically more stable positions combined with annihilation processes) and shows the true depth of the influenced material layer by shot peening. The results presented now allow to judge how far the Almen intensity enables conclusions concerning stress distribution. In principle three properties are of interest in this context, the residual stress value on the surface, the depth and the value of the maximum compressive residual stress and the penetration depth of the compressive residual stresses. A correlation of the Almen intensity with the surface value of the residual stresses does not appear to be useful because the surface value of the residual stresses is not significantly effected by the peening parameters. The depth and the value of the maximum compressive residual stress are certainly not useful, because it is directly on the surface for softer workpiece conditions. The penetration depth drawn only as a function of the Almen intensity as shown in Fig. 15, leads to reasonable correlations. Here the penetration depths and the corresponding Almen intensity can be seen for the normalized, the T450 and the hardened materials conditions in linear relationships, where the penetration depth increase with increasing Almen intensity.

6. Summary

Fig. 16 summarized schematically the influence of the presented peening parameters on the residual stress distribution. The arrows show the shift direction of the residual stress distribution when the indicated parameter increases. It can be seen that an increase of the workpiece hardness HV results in a decrease of the penetration depth of the compressive residual stresses and in a formation of a maximum compressive residual stress value below the surface which also increases with increasing hardness. An increase of the shot hardness HV_{st} effects an increase of the maximum compressive residual stress only for harder material conditions. A growth of the mass flow results in a smaller penetration depth of the compressive residual stresses and, for a coverage below 100%, in an increase of the maximum compressive residual stress. Furthermore a higher peening pressure and a larger shot size causes an increasing penetration depth of the compressive residual stresses and an enlargement of the surface distance of the maximum value of the compressive residual stresses.

Finally there remains to be mentioned that with increasing workpiece hardness the half width values of the surface layers show a transition from microstructural hardening to softening. The peening pressure is not the only parameter which has an decisive effect on the half width values.

Literature

[1] E. Macherauch, H. Wohlfahrt, R. Schreiber at al.: Verbesserung der Bauteileigenschaften durch Strahlen, HFF-Bericht Nr. 6, Umformtechn. Kolloquium Hannover, 12/13.3. 1980

[2] B. Scholtes: Eigenspannungen in mechanisch randschichtverformten Werkstoffzuständen, Ursachen, Ermittlung und Bewertung, Habiliationsschrift Universität Kralsruhe (TH), DGM Informationsgesellschaft 1991

[3] T. Hirsch: Zum Einfluß des Kugelstrahlens auf die Biegeschwingfestigkeit von Titan und Aluminiumbasislegierungen, Dr.-Ing. Dissertation, Universität Karlsruhe (TH), 1983

[4] R. Schreiber: Untersuchungen zum Dauerschwingverhalten des kugelgestrahlten Einsatzstahles 16MnCr5 in verschiedenen Wärmebehandlungszuständen, Dr.-Ing. Dissertation, Universität Karlsruhe (TH), 1976

[5] J. Bernasconi, M. Roth: Residual stress distribution in shot peened plates, BBC-Research-Report, KLR 85-96C, 1985

[6] A. Niku-Lari: Overview on the shot peening process in "Advances in surface treatments" Vol. 5, 155-170, ed. by A. Niku-Lari, Pergamon Press, 1987

[7] R. Schreiber, H. Wohlfahrt, E. Macherauch: Der Einfluß des Kugelstrahlens auf das Biegewechselverhalten von normalgeglühtem 16MnCr5, Arch. Eisenhüttenwes. 48 (1977), 649-652

[8] R. Schreiber, H. Wohlfahrt, E. Macherauch: Zum Einfluß von Kugelstrahlbehandlungen auf das Biegewechselverhalten von einsatzgehärtetem 16MnCr5 im angleassenen Zustand, Arch. Eisenhüttenwes. 49 (1978), 265-269

[9] P. Starker: Der Größeneinfluß auf das Biegewechselverhalten von Ck45 in verschiedenen Wärmebehandlungszuständen, Dr.-Ing. Dissertation, Universität Karlsruhe (TH), 1981

[10] Proc. of the first Int. Conf. on Shot Peening, Paris, 1981, (ed. by A Niku-Lari), Pergamon Press, Oxford, 1982

[11] Proc. of the second Int. Conf. on Shot Peening, Chicago, (ed. by H.O. Fuchs), The American Shot Peening Society, Paramus, New York, 1984

[12] Proc. of the fourth Int. Conf. on Shot Peening, Tokyo, (ed. by K, Iida, The Japan Soc. Precision Engineering, Tokyo, 1990

[13] Proc. of the fifth Int. Conf. on Shot Peening, Oxford, (ed. by D. Kirk), Oxford, 1993

[14] W. Köhler: Influence of shot peening with different peening materials on the stress and corrosion fatigue behavior of a welded AlZnMg-alloy, in [11], 126-132

[15] J.E. Hoffmann: Der Einfluß fertigungsbedingter Eigenspannungen auf das Biegewechselverhalten von glatten und gekerbten Proben aus Ck45 in verschiedenen Wärmeabehandlungszuständen, Dr,-Ing. Dissertation, Universität Karlsruhe (TH), 1984

[16] W. Köhler, B. Scholtes: Einfluß einer Kugelstrahlbehandlung auf die Eigenspannungen einer geschweißten AlznMg-Legierung, in "Eigenspannungen, Entstehung-Messung-Bewertung", Hrsg. V. Hauk, E. Macherauch, DGM 1983, Bd. 2, 331-341

[17] D. Viereck, D. Löhe, O. Vöhringer, E. Macherauch: Influence of shot peening residual stresses on the tensile deformation behavior of NiCr22Co12Mo9, Proc. of the third Int. Conf. on Residual Stress, Tokushima, 1991, (ed by H. Fujiwara, T. Abe, K. Tanaka), Elsevier Applied Science, London, 1992, 766-771

[18] J. Horwath: Effect of shot peening variables on bending fatigue, in [10], 229-236

[19] A. T. DeLitizia: Influence of shot peening on the residual stress in spring steel plate, in [11], 237-240

[20] P. Starker, H. Wohlfahrt, E. Macherauch: Riβentstehung bei Biegewechselbeanspruchung von kugelgestrahltem Ck45 in gehärtetem Zustand, in "Eigenspannungen", DGM (1980), 319-330

[21] R. Schreiber, H. Wohlfahrt, E. Macherauch: Der Einfluß des Kugelstrahlens auf das Biegewechselverhalten von blindgehärtetem 16MnCr5, Arch Eisenhüttenwes. 48 (1977) 12, 653-657

[22] H. Lepand: Änderung des Dauerschwingverhaltens von Federstahl 50Cr4 durch Oberflächenverfestigen mit Strahlmittel verschiedener Härte bie unterschiedlichen Flächenbedeckungen, Dr.-Ing. Dissertation, TH Clausthal, 1965

[23] H. Wohlfahrt: Ein Modell zur Vorhersage kugelstrahlbedingter Eigenspannungs-zästande, in "Eigenspannungen, Entrsthung-Messung-Bewertung", Hrsg. V. Hauk E, Macherauch, DGM (1983) Bd. 2, 301-319

[24] F. Bugahn, O. Vöhringer, E. Macherauch: Microstructural investigation of the shot peened steel 42Cr Mo4 in different heat treatment conditions by the aid of a X-ray profile analysis, in [12], 199-207

[25] K. Iida, K. Tosah: Work-softening induced by shot peening for austenitic stainless steel, in [13], 311-318

[26] E. Macherauch, P. Müller: Das $\sin^2\psi$-Verfahren der röntgenographischen Spannungsmessung, Z. f. angew. Physik 7 (1961) 13, 305-312

[27] M.G. Moore, W.P. Evans: Mathematical corrections for stress in removed layers in X-ray diffraction residual stress analysis, Trans. SAE 66 (1958), 340-345

[28] H. Brugger, E. Macherauch, O. Vöhringer: Eingluß gezielter Wärmebehandlungen von 16MnCr5 auf mechanische Kenngrößen des Zugversuches, HärtereiTechn. Mitt. (1971), 340-353

[29] P. Martin: Beitrag zur Ermittlung der Einflußgrößen beim Kugelstrahlen durch Einzelkornversuche, Dr.-Ing. Dissertation, Hochschule der Bundeswehr, 1980

Tables

Tab. 1: Heat treatment parameters of the investigated samples

Tab. 2: Peening parameters for the investigation of the workpiece hardness on the surface properties

Tab. 3: Peening parameters for the investigation of the shot type on the surface properties

Tab. 4: Peening parameters for the investigation of the peening pressure on the surface properties

Tab. 5: Peening parameters for the investigations of the mass flow on the surface properties

Figures

Fig. 1: Surface roughness R_t before (grinded condition) and after the shot peening treatment (S170 46HRC, p= 1.6 bar, m=1.5 kg/min) vs. workpiece hardness HV0.3

Fig. 2: Residual stress σ^{rs} vs. distance from surface for different heat treatment conditions

Fig. 3: Half width HW of interference lines vs. distance from surface for different heat treatment conditions

Fig. 4: Surface roughness R_t vs. workpiece hardness HV0.3 for different shot types

Fig. 5: Residual stress σ^{rs} vs. distance from surface for different shot types (p = 1.6 bar, m= 1.5 kg/min), quenched and tempered condition T450

Fig. 6: Residual stress σ^{rs} vs. distance from surface for different shot types (p = 1.6 bar, m= 1.5 kg/min), hardened condition

Fig. 7: Surface roughness R_t vs. peening pressure p for different heat treatment conditions (m = 1.5 kg/min)

Fig. 8: Residual stress σ^{rs} vs. distance from surface for different peening pressures (S170 56HRC, m= 1.5 kg/min), normalized condition

Fig. 9: Residual stress σ^{rs} vs. distance from surface for different peening pressures (S170 56HRC, m = 1.5 kg/min), hardened condition

Fig. 10: Half width HW vs. distance from surface for different peening pressures and different heat treatment conditions (m = 1.56 kg/min)

Fig. 11: Surface roughness R_t vs. mass flow m for different heat treatment conditions (p = 3 bar)

Fig. 12: Residual stress σ^{rs} vs. distance from surface for different mass flows m (S170 46HRC, p = 3 bar), quenched and tempered condition T 450

Fig. 13: Residual stress σ^{rs} vs. distance from surface for different mass flows m (S170 56HRC, p = 3 bar), hardened condition

Fig. 14: Residual stress σ^{rs} vs. surface distance for different mass flows m and exposure times, (coverage = const., S170 46HRC, p = 3 bar), normalized condition

Fig. 15: Penetration depth of the compressive residual stresses vs. Almen intensity for different heat treatment conditions

Fig. 16: Influence of the peening parameters on the residual stress distribution (schematically)

Tables and Figures on pages 11-13

Designation	Heat treatment	Hardness
normalized	930 °C / 3h, furnace cooling	HV 230
T 650	850 °C / 20 min - oil 25 °C + 650 °C / 2h, furnace cooling	HV 295
T 450	850 °C / 20 min - oil 25 °C + 450 °C / 2h, furnace cooling	HV 430
T 300	850 °C / 20 min - oil 25 °C + 300 °C / 2h, furnace cooling	HV 525
T 180	850 °C / 20 min - oil 25 °C + 180 °C / 2h, furnace cooling	HV 600
hardened	850 °C / 20 min - oil 25 °C	HV 660

Tab. 1

Shot type	S 170
Hardness [HRC]	46
Peening pressure [bar]	1.6
Mass flow [kg/min]	1.5
Almen intensity [mmA]	0.3

Tab. 2

Shot type	Peening pressure [bar]	Mass flow [kg/min]	Almen intensity [mmA]
S110 46HRC	1.6	1.5	0.20
S170 46HRC			0.30
S170 56HRC			0.31
S330 56HRC			0.50

Tab. 3

Heat treatment	Shot type	Peening pressure [bar]	Mass flow [kg/min]	Almen intensity [mmA]
normalized	S170 46HRC	1.6	1.5	0.3
T 650		5		0.59
T 450		8		0.68
T 300	S170 56HRC	1.6	1.5	0.31
T 180		5		0.61
hardened		8		0.70

Tab. 4

Heat treatment	Shot type	Mass flow [kg/min]	Peening pressure [bar]	Almen intensity [mmA]
normalized	S170 46HRC	1.5	3	0.44
T 650		6		0.35
T 450		10		0.35
T 300	S170 56HRC	1.5	3	0.47
T 180		6		0.38
hardened		10		0.36

Tab. 5

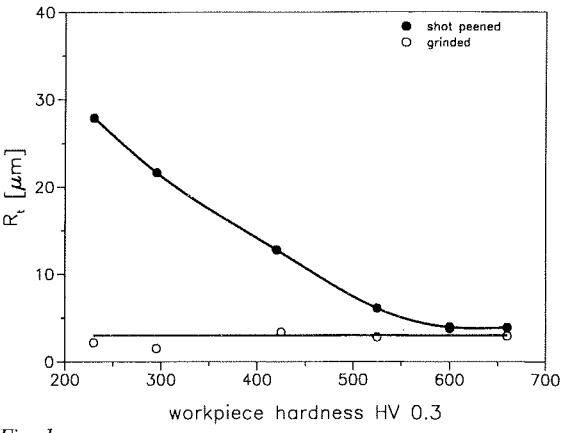

Fig. 1

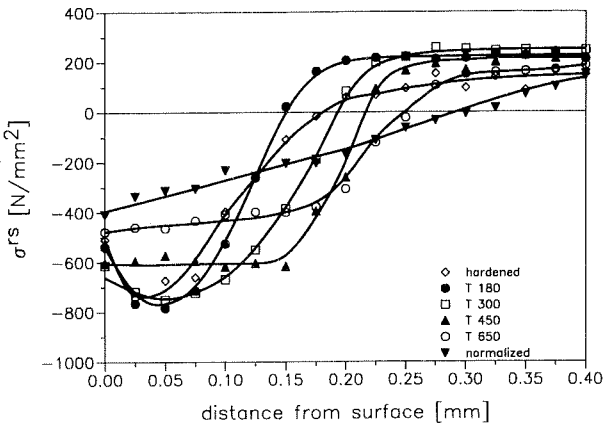

Fig. 2

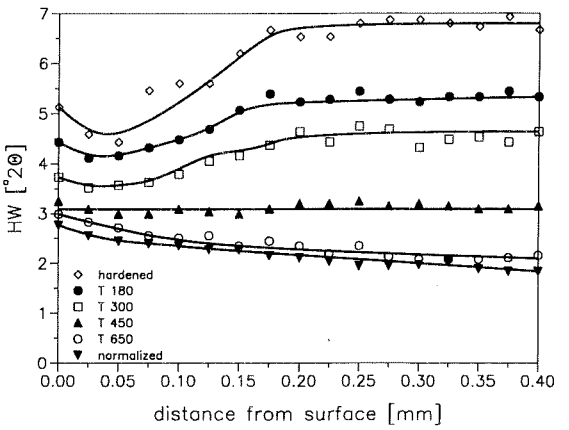

Fig. 3

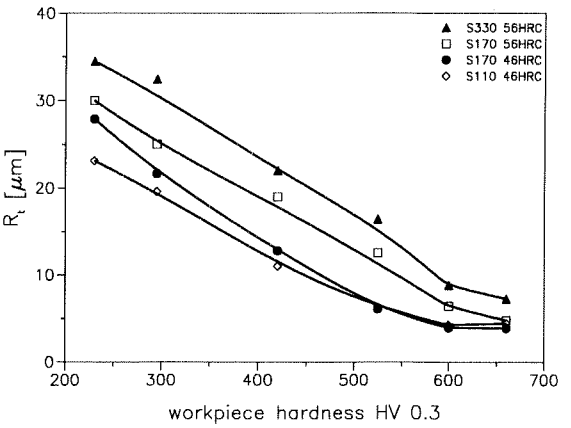

Fig. 4

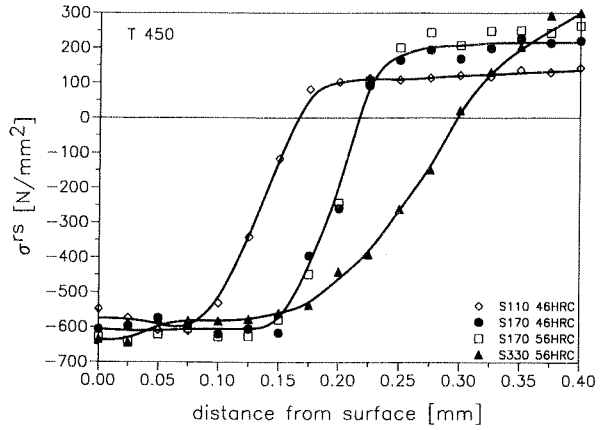

Fig. 5

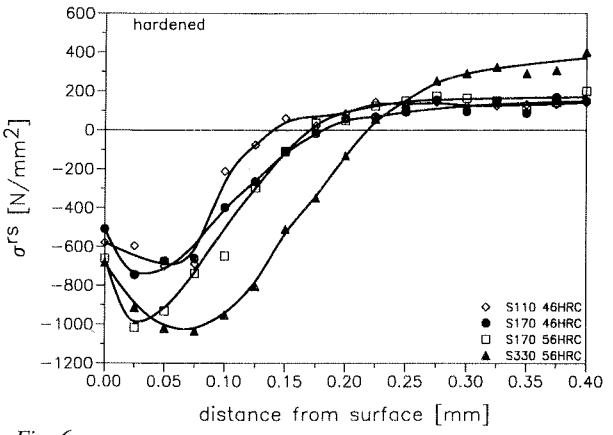

Fig. 6

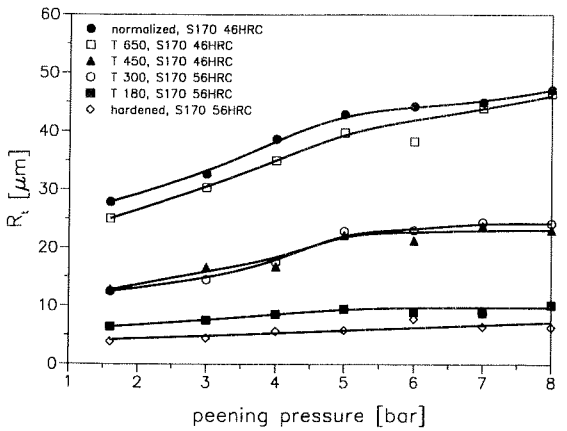

Fig.7

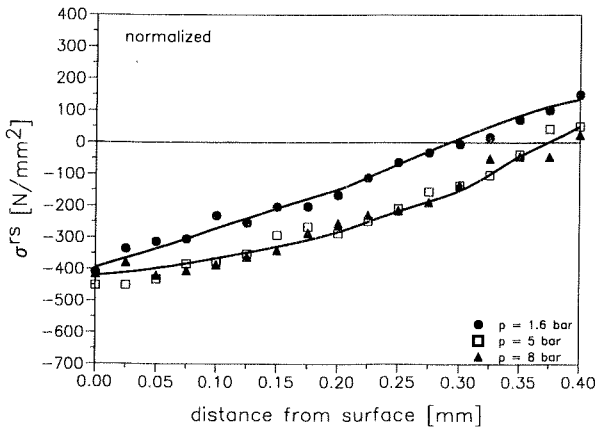

Fig. 8

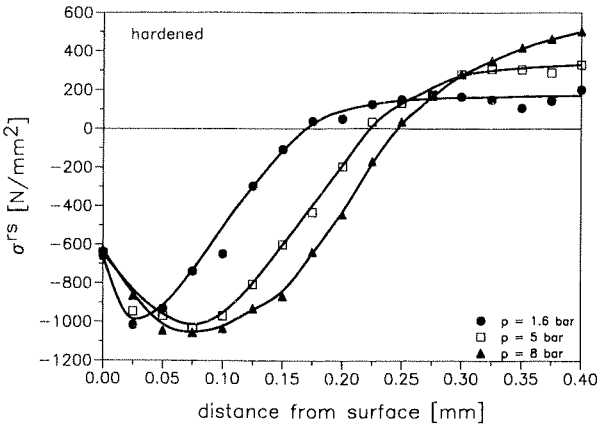

Fig. 9

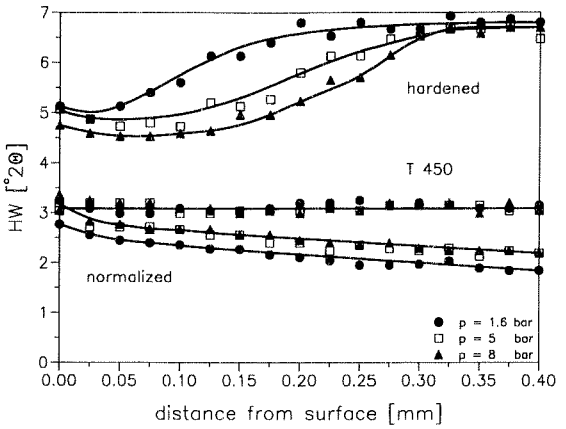

Fig. 10

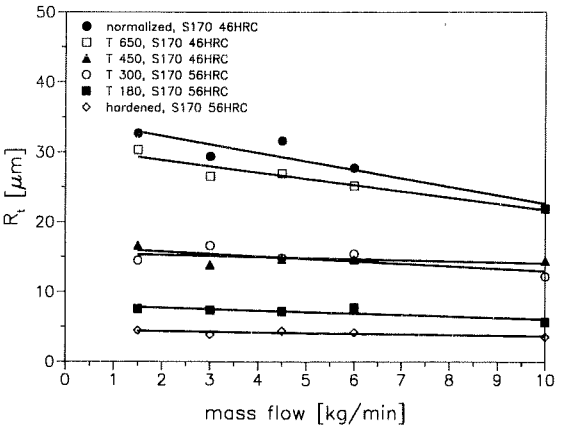

Fig. 11

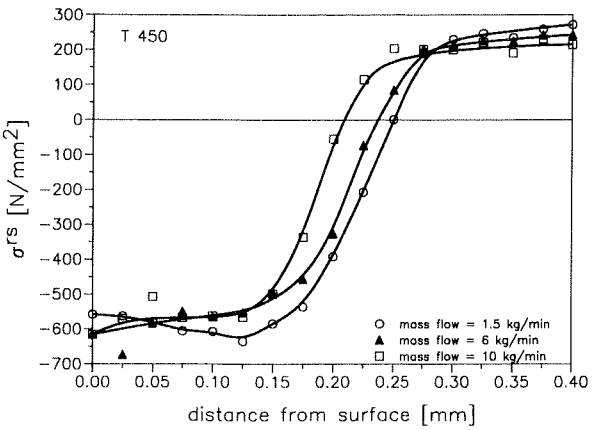

Fig. 12

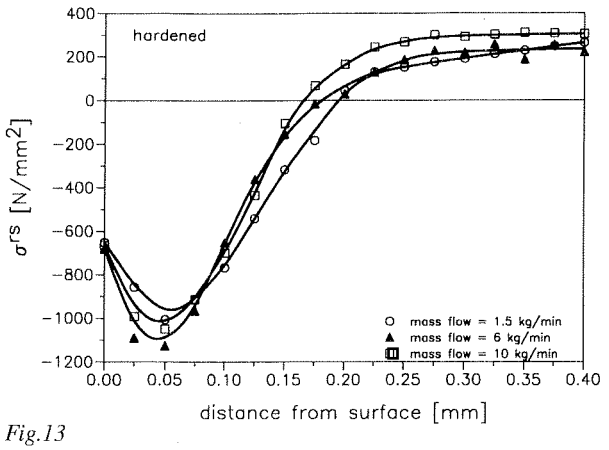

Fig.13

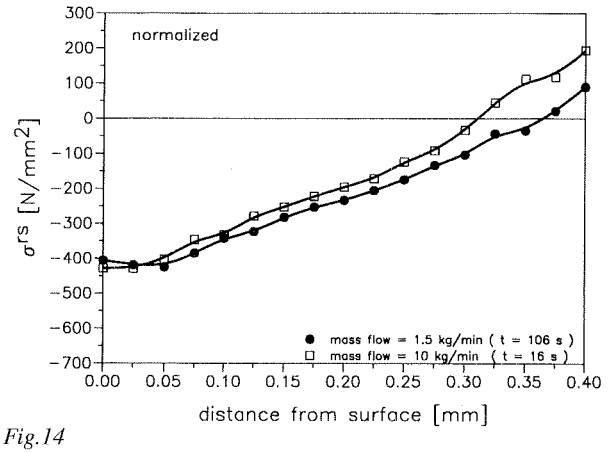

Fig.14

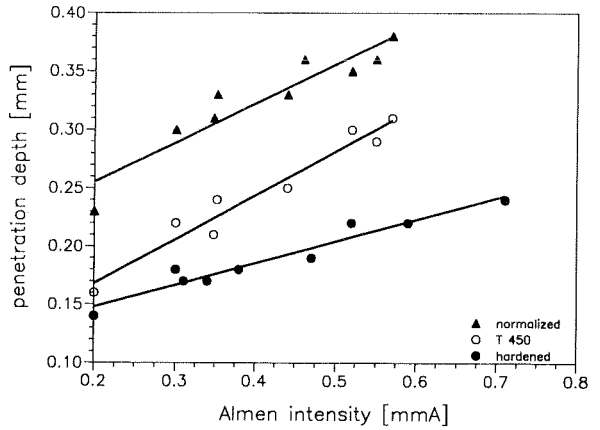

Fig.15

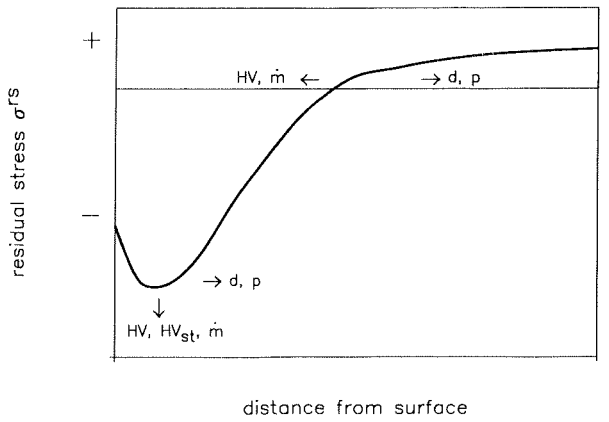

Fig.16